Enhancing the efficiency of an axial impulse turbine with a diffuser

Geetam Saha, Diogo Neves Ferreira, Narasimalu Srikanth and Lei Zuo

Abstract—**In oscillating water column wave energy converters, the aerodynamic losses caused by flow misalignment between the rotor outlet and the outlet guide vane of self-rectifying impulse turbines are a significant design problem. The symmetrical positioning of guiding vanes on both sides of the rotor is the reason for it. In comparison to the equivalent Wells turbine, the efficiency of impulse turbines is lower because of these losses in the outlet guide vane. This paper presents a strategy to develop an improved design of an axial impulse turbine to reduce the losses in the outlet guide vane along with the residual kinetic energy loss by integrating a diffuser between the rotor and guide vanes. The proposed model was investigated numerically using RANS simulations. Multiple diffuser geometries were tested against the reference turbine for comparison of the performance characteristics. The results support the hypothesis behind the proposed design. The performance was compared extensively with the reference case in terms of the dimensionless loss coefficients for a better insight into the contribution of all the turbine sectors. The current work shows a possible design path for the performance improvement of the turbine. Results also support the fact that the guide vanes need to be redesigned for obtaining maximizing efficiency with the proposed design. The losses in the outlet guide vane were reduced by approximately 50% with an overall efficiency rise of around 2%.**

Keywords—**Oscillating Water Column, Wave Energy, Impulse Turbine, Self-Rectifying Turbines.**

I. Introduction

THE self-rectifying turbines have significant importance for the optimal design of oscillating water column (OWC) wave energy converters (WEC). Self-rectifying turbines have unique characteristics of operation in the same rotational direction irrespective of the direction of the airflow through the turbine. These kinds of turbines are highly appreciated in OWC applications because they eliminate the use of bypass and relief valves for continuous energy extraction [1]. High volume flow rate and shorter time periods were the key challenges for the assemblies with conventional turbines with valves for OWC WEC applications [2]. In the energetic sea states, the functioning and performance of the valves were inferior because of choking and minimal response time [3].

Wells Turbine, invented by Dr. Alan Wells in 1976 is one of the most widely used air turbines because of its geometrical simplicity and high peak efficiency [4]. Wells turbine has been utilized for application in a number of OWC plants across the world such as LIMPET [5]. But with time researchers have come across several problems associated with the Wells turbine when utilized for large-scale applications. These include high tip speed [6], abrupt drop in efficiency [7], high run-away speed [8], inferior noise characteristics [9], hysteresis [10], and poor starting characteristics [11]. Literature also shows the fact that even though the instantaneous peak efficiency is significantly high, the average efficiency under stochastic sea conditions is way lower [12]. In order to resolve all issues, researchers have developed a variety of air turbines with improved performance. A bidirectional impulse turbine (BDIT) is one of the most distinguished turbines which have also been adopted for applications in OWC WEC by the marine energy community. The key advantage of BDIT is the broad operational bandwidth which is of prime importance for operations in stochastic and energetic sea conditions [13]. In addition to the absence of stall characteristics, BDIT has an excellent starting performance with a significantly low runaway speed [14]. For offshore and mobile applications, this absence of the requirement for startup is a key advantage. BDIT despite having multiple advantages has a major fallacy, which is the lower peak efficiency [15]. The reason behind the lower peak efficiency is the misalignment between the fluid flow from the rotor outlet and the outlet guide vanes [16]. In the case of BDITs, this problem is inherited because of the identical geometry of both the guide vanes to operate in reciprocating flows. The flow misalignment results in a high incidence angle at the outlet guide vane causing severe flow separation which leads to high stagnation pressure losses. Scientific literature suggests that researchers have investigated this problem of flow obstruction and have attempted to address it by utilizing different design strategies.

Setoguchi et al. proposed the integration of variable guide vanes for the reduction of flow obstruction. The pair of guide vanes were pivoted and made free to align themselves with the flow by the action of aerodynamic moments and were constrained to mechanical stops at two prefixed angles [17]. The peak

Geetam Saha is with the Department of Mechanical Engineering, Virginia Polytechnic Institute and State University, Blacksburg, VA, 24060, USA (e-mail: sahageetam@vt.edu).

Diogo Neves Feriera is with IDMEC, Instituto Superior Tecnico, Universidade de Lisboa, Av. Rovisco Pais 1, 1049-001, Lisboa, Portugal (e-mail: nevesferreira@tecnico.ulisboa.pt).

Narasimalu Srikanth is with Energy Research Institute @ NTU, Nanyang Technological University, Singapore, 637141, Singapore (e-mail: nsrikanth@ntu.edu.sg).

Lei Zuo is with the Department of Naval Architecture and Marine Engineering, University of Michigan, Ann Arbor, MI, 48109, USA (e-mail: leizuo@umich.edu).

Digital Object Identifier:
https://doi.org/10.36688/ewtec-2023-185

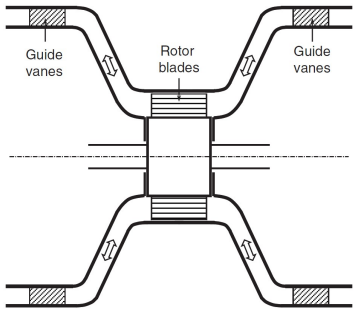

Fig. 1. Scehmatic representation of impulse turbine with radially and axially offset guide vanes (reproduced from [2]).

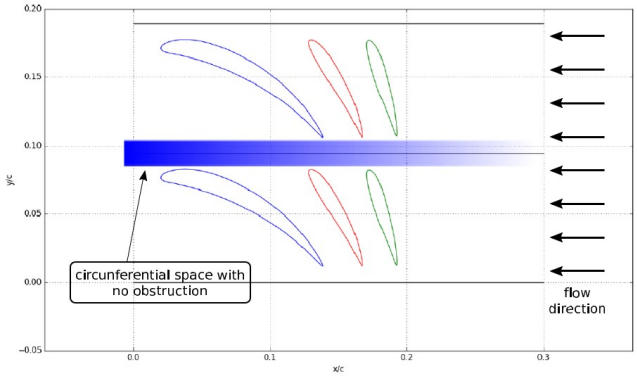

Fig. 2. Reduction of obstruction in axial direction (reproduced from [21]).

efficiency was improved considerably but the design added mechanical complexity resulting in maintenance and reliability concerns for prolonged applications. The losses were also investigated by utilizing smaller values of absolute flow deflection from the inlet guide vane for reducing blockage, but this resulted in inferior performance of the turbine because of reduced momentum transfer to the rotor blade from the fluid flow [18].

Another approach suggested by researchers was the reduction of the flow speed at outlet guide vanes in order to reduce the stagnation pressure losses [2]. HydroAir turbine was based on the strategy of minimizing the losses by reducing the flow speed from the rotor outlet by radially and axially offsetting the guide vanes from the rotor blades [19], see Fig.1. The offsets resulted in the reduction of the circumferential and the meridional velocity which translated to reduced kinetic energy at the outlet guide vanes. This configuration of the turbine was considerably bulky.

A concentric guide vane row topology vanes was proposed by Kymaner (Portuguese company) for loss reduction. The novel design divided the flow deflection into multiple rows for distributing the aerodynamic load on each row resulting in the reduction of tangential chord length [20]. This configuration increased the unhindered flow passage for the outflow from the rotor, (Fig. 2). The efficiency of the turbine was improved by reducing the stagnation pressure losses.

Open literature suggests that out of all the bidirectional impulse turbines available, the biradial turbine has the best performance characteristics. A comparison

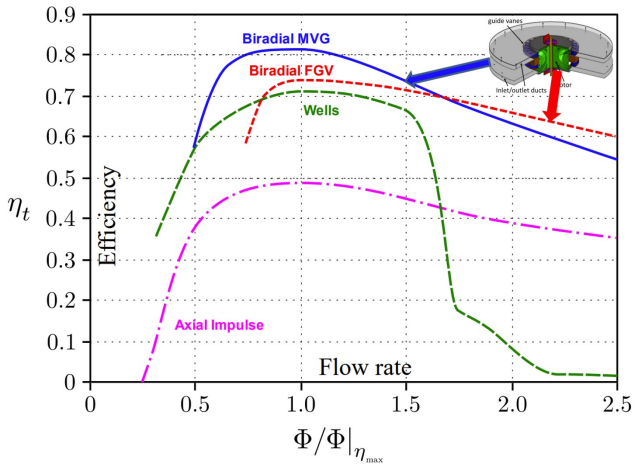

Fig. 3. Comparison of the biradial turbine with other types of air turbine (MGV: Moving Guide vane, FGV: Fixed Guide Vane) [22] [23].

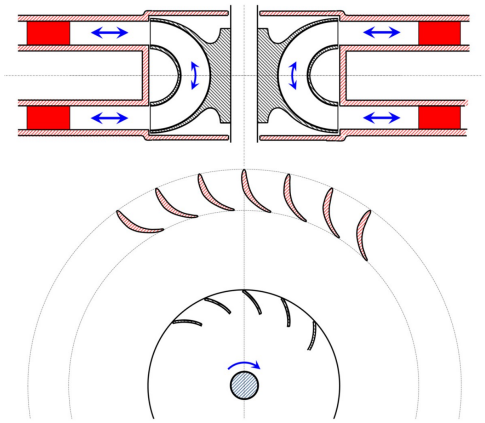

Fig. 4. Schematic representation of biradial turbine with fixed guide vanes (reproduced from [24]).

of the performance of the biradial turbine with the other types of air turbine is presented in Fig. 3 [22], [23]. Falaco et al. developed the biradial turbine in 2012 [24]. A primary objective behind the design was to propose an efficient design as an alternative to the self-rectifying axial impulse turbine which is capable to deal with the aerodynamic stalling losses due to the flow misalignment in the outlet guide vanes. The schematic description of the biradial turbine is shown in Fig. 4. A biradial turbine is an impulse turbine that is symmetric with respect to the plane perpendicular to the axis of rotation and operates under centrifugal and centripetal modes. The guide vanes are radially offset from the rotor and are connected through axisymmetric ducts to the corresponding rotor inlet/outlet [25]. By virtue of this design, the circumferential and the radial components of the rotor outflow are minimized resulting in reduced stagnation pressure losses at the outlet guide vanes. This reduction in losses increases the turbine efficiency appreciably. Despite the higher efficiency, the challenge lies in the complexity and intricate design of the turbine assembly. The biradial turbine configuration involves more complex design and manufacturing processes compared to simpler turbine designs.

TABLE I
REFERENCE GEOMETRY PARAMETERS [26].

Parameter	Specification
Number of Rotor Blades	30
Number of Guide Vanes	26
Hub Diameter	210 mm
Tip Diameter	298 mm
Tip Clearance	1 mm
Rotor Blade Chord Length	54 mm
Guide Vane Chord Length	70 mm
Rotor Blade Inlet Angle	60°
Guide Vane Setting Angle	30°
Rotor Blade Pitch	26.7 mm
Guide Vane Pitch	30.8 mm

This paper introduces a diffuser for axial impulse turbines located between the rotor and the downstream guide vanes. The research objective is to increase the efficiency of the reference axial turbine [26] with a simpler and more compact design compared to the HydroAir and biradial turbines. Like in these designs, efficiency gains results from the reduction of the flow kinetic energy before reaching the downstream guide vanes. The main contributions of this research are the validation of the design approach through Computational Fluid Dynamics simulations and the identification of pathways for further enhancement.

The remainder of this paper is organized as follows. Section III validates of the numerical tools with the experimental results of the reference case and presents its performance enhancement from the integration of the proposed diffuser design. Design challenges are also identified and discussed in this Section. Section IV summarizes the outcomes of the research and establishes the research paths for further design improvements.

II. METHODOLOGY

A. Reference Turbine Test Case

The fixed geometry impulse turbine design by Maeda et al. [26] was considered in the present study. The geometrical details of the rotor and the guide vanes are shown in Fig. 5. The rotor blade profile consists of an elliptical arc on the suction side and a circular arc on the pressure side with a leading and trailing edge radius of 0.5 mm. The entry and exit angles of the rotor blade are $60°$. The guide vane profile consists of a straight line and a circular arc with a camber and settling angle of $60°$ and $30°$ respectively. The hub-to-tip ratio of the reference turbine was 0.7. The details of the geometrical parameters of the turbine are presented in Table I.

Maeda et al. experimentally investigated the reference turbine with a 300 mm diameter in a piston cylinder test rig under steady-state flow conditions. The performance of the turbine was described by them in terms of angular velocity, average torque, flow rate, and total pressure drop. The Reynolds number based on the relative inflow velocity [27] and the blade chord length was approximately equal to 40,000 at the peak efficiency. In the current work, the computational setup was validated against the same flow conditions for the reference turbine.

B. Diffuser design

The proposed design is an annular diffuser connecting the rotor outlet section to the inlet of the downstream guide vanes. The diffuser decreases the rotor outflow axial velocity which has two beneficial effects on the turbine efficiency. The first is the decrease of stagnation pressure losses on the outlet guide vanes since these losses are directly proportional to the kinetic energy of the incoming flow. The second is the decrease of the wasted flow kinetic energy at the turbine outlet, which is characteristic of OWC converters.

Fig. 6 and Fig. 7. present the schematic representation of the typical axial BDIT and the proposed design respectively. In Fig. 7, sectors 2-3 and 4-5 represent the nozzle and diffuser respectively. The rotor blade span and the guide vanes mean radius in the proposed design are kept equal to the reference case with the objective to maintain a compact turbine.

The diffuser geometry was parameterized based on its axial length, L, and cant angles, ε, of the hub and shroud as shown in Fig 8. The turbine symmetry with respect to a plane perpendicular to the rotor axis was kept. As such, equal diffuser geometries were added to both rotor sides, each behaving as a nozzle or diffuser depending on the flow direction.

Four turbines with different diffuser/nozzle pairs were investigated in the present work. The rotor, guide-vane geometries, and mean radius were kept from the reference case and the diffusers were designed as follows. A diffuser cant angle, ε, was chosen and the initial length, L, equal to the reference case was set. While no boundary layer separation was detected on the diffuser, its length was increased up to the onset of separation. The objective was to obtain the longest diffuser possible for different cant angles keeping the boundary layer attached.

C. Performance Metrics

The numerical validation of the reference geometry was based on the metrics introduced by Maeda et al. [26] assuming incompressible flow across the turbine, defined here as follows.

The flow coefficient is

$$\phi = \frac{V_z}{U_m}, \tag{1}$$

where V_z is the axial component of the velocity at the rotor inlet (note that it is equal to the rotor outlet axial velocity due to mass flow conservation), U_m is the transport velocity at the mean radius, defined by $U_m = \Omega R_m$, where Ω is the rotational speed, R_m is the rotor blade mean radius.

The torque coefficient is defined as

$$C_t = \frac{2T}{\rho(V_z^2 + U_m^2) b\, l Z R_m} \tag{2}$$

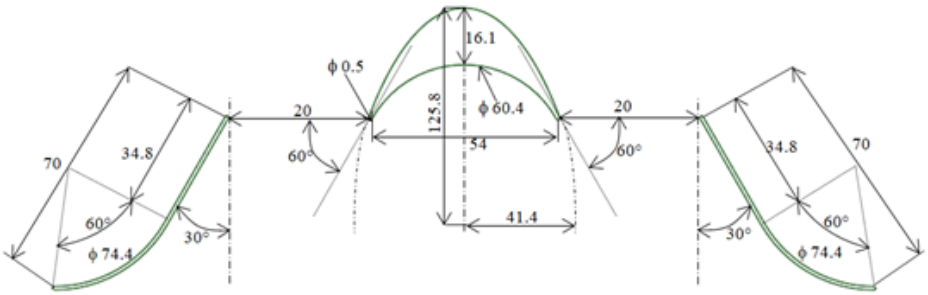

Fig. 5. Reference case blade geometry.

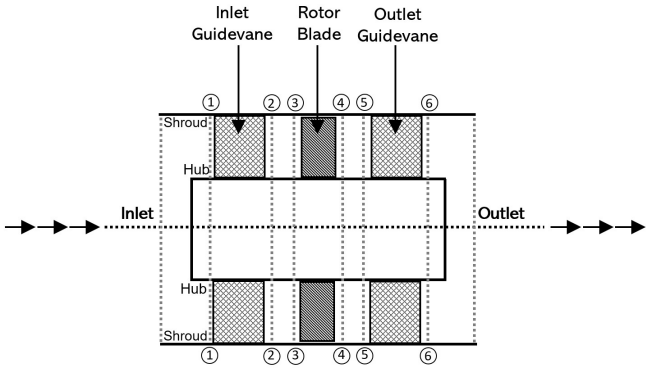

Fig. 6. Reference turbine meridional view.

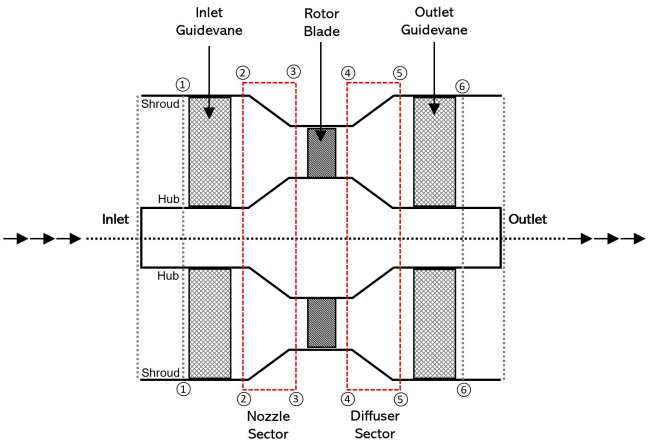

Fig. 7. Proposed design meridional view.

where T is the rotor torque, ρ is the air density at the turbine inlet, b is the rotor blade height and Z is the number of blades.

The input coefficient is

$$C_{\mathrm{a}} = \frac{Q(p_{0_1} - p_6)}{\rho(V_{\mathrm{z}}^2 + U_{\mathrm{m}}^2) b\, l Z V_{\mathrm{z}}}\,, \tag{3}$$

where Q is the flow rate into the turbine, p_{0_1} is the stagnation pressure at the turbine inlet (section 1) and p_6 is the pressure at the turbine outlet (section 6). Note that the turbine outflow kinetic energy, $p_{0_6} - p_6$, is wasted.

The performance assessment of the proposed design is based on the metrics defined by Falcao [24]. They are defined as follows.

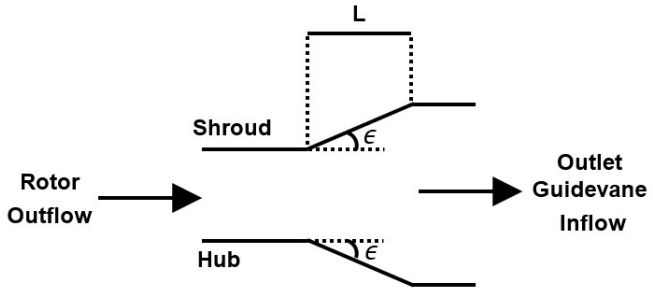

Fig. 8. Diffuser design variables.

The flow rate coefficient is

$$\Phi = \frac{Q}{\Omega D^3}\,, \tag{4}$$

where D is the rotor diameter.

The pressure head coefficient, also known as the total-to-static pressure coefficient is

$$\Psi_{\mathrm{ts}} = \frac{p_{0_1} - p_6}{\rho \Omega^2 D^2}\,. \tag{5}$$

The torque coefficient is

$$\Pi = \frac{T}{\rho \Omega^2 D^5}\,. \tag{6}$$

The turbine to total-to-static efficiency is the ratio of the mechanical power to the pneumatic power. It can be calculated with either family of dimensionless coefficients by

$$\eta_{\mathrm{ts}} = \frac{C_{\mathrm{t}}}{\phi C_{\mathrm{a}}} = \frac{\Pi}{\Phi \Psi_{\mathrm{TS}}}\,. \tag{7}$$

Losses in a turbine sector between two sections i, j other than the rotor, $i, j = 3, 4$, as illustrated in Figs. 6 and 7, are assessed using the loss coefficient,

$$\lambda_{i,j} = \frac{p_{0_i} - p_{0_j}}{\frac{1}{2}\rho V_{\mathrm{z}}^2}\,, \tag{8}$$

where the denominator is a reference kinetic energy based here on the axial mean velocity at the rotor inlet. Not all the stagnation pressure variation in the rotor sector corresponds to a loss since part of it is converted into mechanical energy. As such the rotor loss coefficient is

$$\lambda_{3,4} = \frac{p_{0_3} - p_{0_4} - \frac{\Omega T}{Q}}{\frac{1}{2}\rho V_{\mathrm{z}}^2}\,. \tag{9}$$

The kinetic energy associated with the flow at a given section in dimensionless form is given by the kinetic energy coefficient,

$$K_i = \frac{p_{0_i} - p_i}{\frac{1}{2}\rho V_z^2}\,. \tag{10}$$

The coefficients defined in (8) to (10) are useful to compare the performance of two sectors from different turbines, e.g. the losses in two diffusers. To assess a sector's losses relative to a turbine total pressure head, the relative loss coefficients are used.

The relative losses in a turbine sector other than the rotor are

$$\Lambda_{i,j} = \frac{p_{0_i} - p_{0_j}}{p_{0_1} - p_6}\,. \tag{11}$$

At the rotor they are

$$\Lambda_{3,4} = \frac{p_{0_3} - p_{0_4} - \frac{\Omega T}{Q}}{p_{0_1} - p_6}\,. \tag{12}$$

Likewise, the kinetic energy loss with the turbine outflow relative to the pressure head is

$$\Lambda_{6\mathrm{k}} = \frac{p_{0_6} - p_6}{p_{0_1} - p_6}\,. \tag{13}$$

The relative loss coefficients are related with the turbine total-to-static efficiency by

$$\sum_{i=1}^{6} \Lambda_{i,i+1} + \Lambda_{6\mathrm{k}} + \eta_{\mathrm{ts}} = 1 \tag{14}$$

D. Numerical Setup

In the current work, 3D RANS (Reynolds Averaged Navier Stokes) simulations were performed using the widely used commercial turbomachinery CFD code CFX® 20.1. CFX® is based on a cell-centered finite volume approach for spatial discretization. All the simulations were performed in steady-state conditions and assuming the working fluid as an ideal gas. Based on the simulation conditions, k-ω shear stress transport turbulence model was used with 5% turbulence intensity. For the simulation of the BDIT, the computational domain was divided into 3 subdomains. They are stationary inlet guide vane, moving rotor blade, and stationary outlet guide vane. The mixing plane approach was used for interfacing the guide vanes subdomains with the rotor blade subdomain. Fig. 11., presents the boundary conditions imposed for the numerical solutions. The pitch ratio used for mixing plane interface 1 and 2 were 0.86 and 1.15 respectively. No slip wall boundary condition was imposed on the hub, shroud, and blade surfaces. A high-resolution unstructured mesh was utilized in the current work with prism layers on the blade surfaces, hub, and shroud. Fig. 9. presents the mesh involved in the simulations.

III. Results and Discussion

A. Validation

In the current work, the numerical results for the reference turbine were compared with the experimental results of Maeda et al. [23] in terms of the turbine efficiency against the flow coefficient ranging from 0.5 to 2.5 at equally spaced intervals, as illustrated in Fig. 11. It can be seen that the results matched considerably with the experimental results within an acceptable tolerance range validating the numerical methods and respective parameters chosen.

TABLE II
Diffuser design results.

ϵ [°]	L/b [-]	L [mm]	Area Ratio [-]
0	0	0	1.0
5	1.6	70.4	1.49
7.5	1.3	57.2	1.56
12.5	0.68	30	1.52
15	0.56	25	1.52

The reference turbine losses distribution relative to the total pressure head are illustrated in Fig. 12. It is observed for the design point, $\phi \approx 0.195$, that outlet guide vane losses amount to 23% of the available pressure head and the inlet guide vanes amount to 3%. This result indicates that improvements to guide vane geometry should aim to reduce the losses of the outlet vanes or of other components, namely the rotor, which are $\Lambda_{3,4} \approx 0.26$. The losses on the outlet guide vanes and the outflow kinetic energy lost collectively amount to 37% of the total available pressure head, justifying the objectives of the present research.

B. Proposed design

Four diffusers were designed following the procedure described in Section II-B for cant angles $5° < \varepsilon < 15°$. It was observed during the design cycles that the flow is prone to separation at the diffuser hub due to low rotor outflow momentum in this area. This was a limiting factor on the diffuser length, L, and as such over the pressure recovery. The four diffusers' geometric parameters are listed in Table II.

The four diffuser-integrated BDIT geometries were compared against the reference case for similar flow rate coefficients. The four efficiency curves are illustrated in Fig. 13. It is noticeable that the turbine efficiency curves follow the same trend regarding changes to the flow rate coefficient. Only the diffuser-integrated design with $\varepsilon = 7.5°$ deviates from the trend at $\phi = 2.0$. It can be seen that for the diffusers with $\varepsilon = 5°$ and $\varepsilon = 7°$ the turbines depict lower efficiency over the entire bandwidth of flow conditions whereas turbines with $\varepsilon = 12.5°$ and $\varepsilon = 15°$ have a superior performance in comparison to the reference turbine. From the two, the turbine with $\varepsilon = 12.5°$ exhibits higher peak efficiency but lower performance at low flow rates.

Considering that all the diffuser-integrated designs should decrease the kinetic energy at sections $i = 5$ and potentially increase the turbine efficiency, individual sector losses, $\lambda_{i,j}$, in all four cases and reference one are listed in Table III alongside the kinetic energy, K_i, at relevant sections for further analysis. It is seen that the the kinetic energy at section $i = 5$ is in fact lower than the reference case for all diffuser-integrated geometries, resulting in significant reduction in downstream guide vane losses, $\lambda_{5,6}$ and wasted turbine outflow kinetic

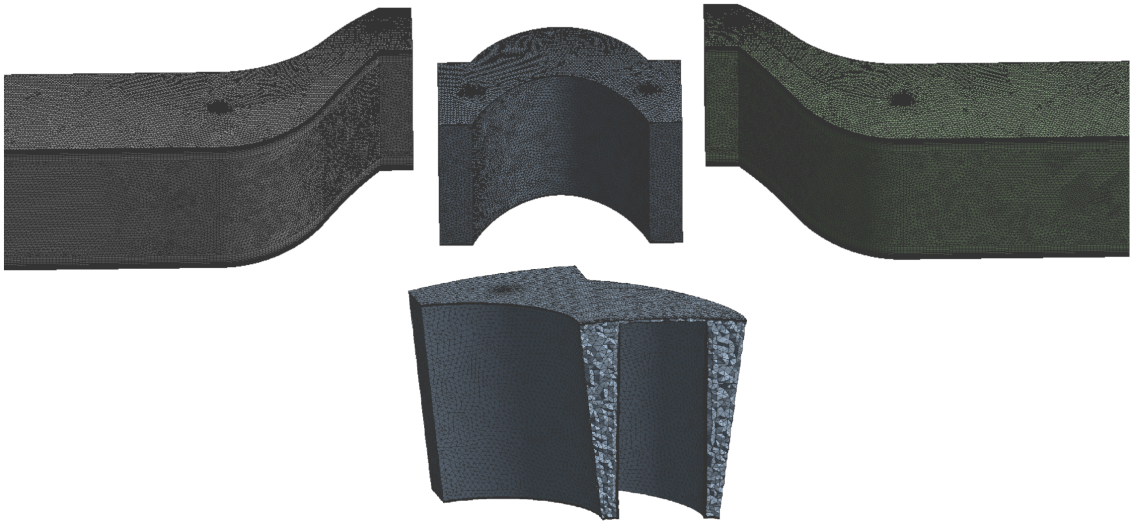

Fig. 9. Reference case mesh.

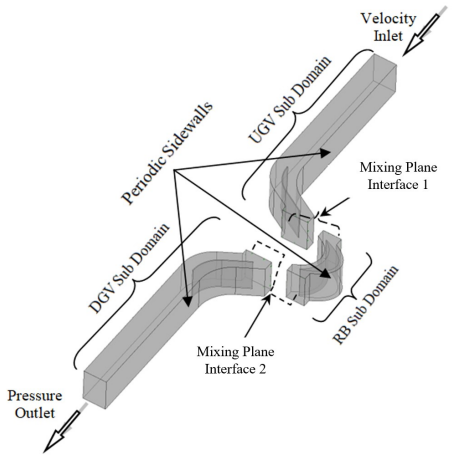

Fig. 10. Simulation setup.

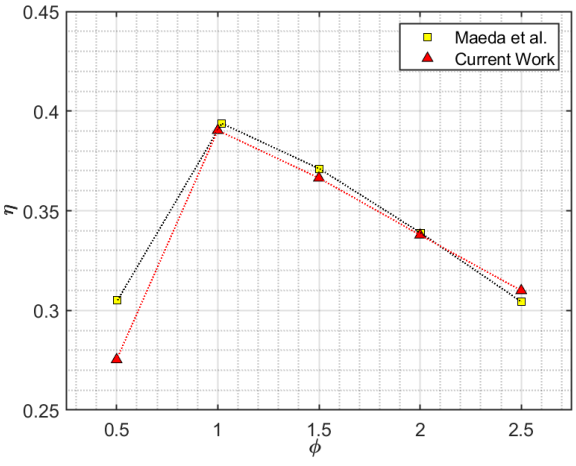

Fig. 11. Validation with Experimental Results

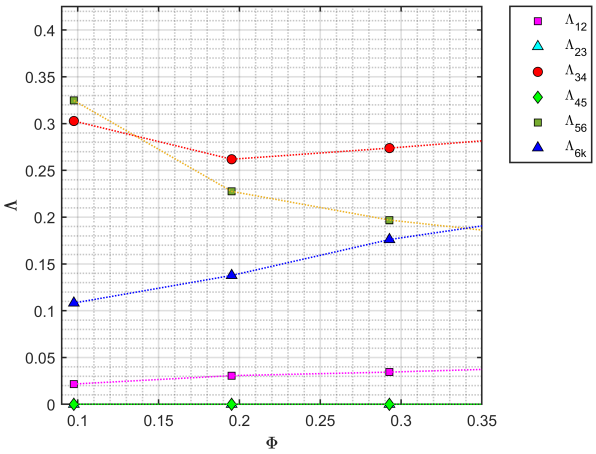

Fig. 12. Relative loss coefficients for the reference turbine.

TABLE III
LOSSES IN EACH TURBINE SECTOR AND KINETIC ENERGY AT RELEVANT SECTIONS.

ϵ	λ_{12}	λ_{23}	λ_{34}	λ_{45}	λ_{56}	K_4	K_5	K_6
0°	0.42	0.00	8.37	0.00	3.15	2.25	2.25	1.91
5°	0.32	0.32	8.45	0.21	1.48	2.12	1.59	1.32
7.5°	0.26	0.26	8.82	0.19	1.19	2.20	1.64	1.11
12.5°	0.24	0.24	8.32	0.05	1.46	2.04	1.59	1.09
15°	0.26	0.26	8.42	0.11	1.40	2.09	1.62	1.19

energy, K_6. But it can also be observed that the designs $\varepsilon = 5°$ and $\varepsilon = 7°$ have increased rotor losses, $\lambda_{3,4}$.

A possible reason behind the increase in rotor losses for all diffuser integrated cases is due to changes in the rotor absolute flow angle induced by the nozzle, $(i, j) = (2, 3)$. Defining the absolute flow angle with respect to the axial direction, at a section i it is $\alpha_i = V_{\theta_i}/V_{z_i}$. Then due to mass conservation V_{z_i} increases from $i = 2$ to $i = 3$.

For completeness, the losses on the sectors of the diffuser-integrated turbine design with $\varepsilon = 12.5°$ is plotted in Fig. 14. As intended, the ratio of the cumulative losses in the outlet guide vanes and turbine outflow to the turbine pressure head have decreased from $\Lambda_{4,6k} = 0.37$ in the reference case (see Fig. 12) to $\Lambda_{4,6k} = 0.23$. On the downside, the rotor losses increased from $\Lambda_{3,4} = 0.26$ to $\Lambda_{3,4} = 0.34$ limiting the potential gains from these particular diffuser-integrated designs. Nevertheless, a total efficiency gain

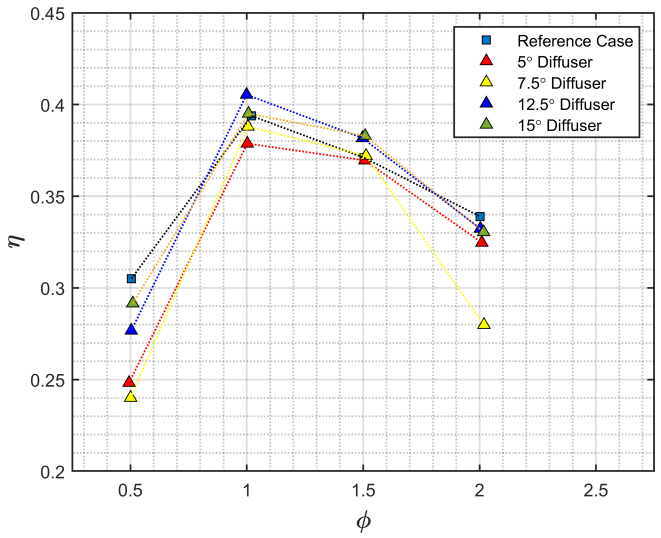

Fig. 13. Efficiency comparison between the diffuser-integrated geometries and the reference case.

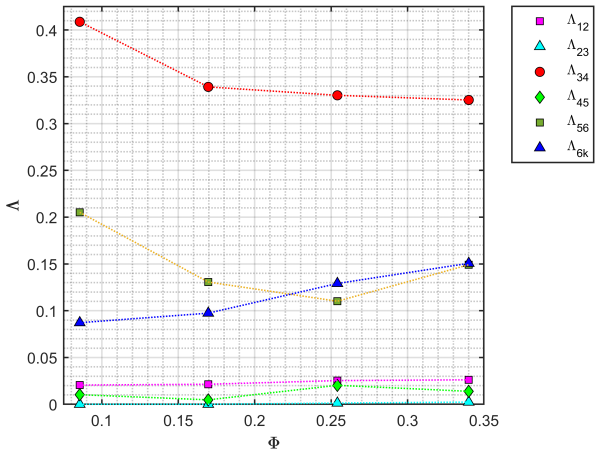

Fig. 14. Relative loss coefficients for the diffuser integrated turbine

of almost 2% was achieved.

IV. Conclusion

This paper introduces an annular diffuser for a well-known axial impulse turbine geometry available in the open literature. The design choices are aimed at increasing the efficiency of the starting geometry and keeping the overall turbine compact when compared to existing models with integrated diffusers. The design objectives were implemented by keeping the diffuser mean radius constant while increasing the meridional channel height. Several diffuser-integrated turbines were simulated using Computational Fluid Dynamics methods and their performances were assessed. The design method achieved its goal of obtaining a turbine geometry with increased efficiency while being compact. Nevertheless, while the losses at the downstream guide vanes were reduced in 50%, the turbine efficiency gains were only around 2% despite the losses in the downstream guide vanes representing 37% of the original turbine pressure head. The efficiency gain was penalized by the reduction of the flow absolute angle induced by the converging nozzle which decreased rotor performance. To take advantage of diffuser-integrated axial impulse turbines, the guide vane deflection must also be adjusted at every design iteration in order to keep a good rotor performance.

Acknowledgements

This research is supported by the funding provided through the NSF grant 1738689. We would also like to thank Mr. Matthew Brown at ARC, Virginia Tech for helping us run the simulations on HPC clusters.

Appendix

TABLE IV
Nomenclature.

Symbol	Description
ϕ	Flow Coefficeint
V_z	Axial Velocity (m/s)
U_{mean}	Angular Velocity at Mean Radius (m/s)
C_t	Torque Coefficeint
T	Torque (Nm)
ρ	Density of working fluid (kg/m^3)
b	Rotor Blade Height (m)
l	Chord Length of Rotor Blade (m)
Z	Number of Rotor Blades
R_m	Mean Radius of Rotor Blade (m)
Δp	Total to Static Pressure Drop (Pa)
Q	Volume Flow Rate (m^3/s)
Φ	Flow Rate Coefficient
ω	Rotational Velocity (rad/s)
p	Static Pressure (Pa)
p_0	Total Pressure (Pa)
ψ_{ts}	Total to Static Pressure Coefficient
π	Turbine Power Coefficient
η_{TS}	Total to Static Efficiency
Λ	Relative Pressure Coefficient
λ	Pressure Coeffcient
V_{ref}	Reference Velocity (m/s)
A	Cross Section Area of Rotor Inlet (m^2)

References

[1] A. F. Falcão and J. C. Henriques, "Oscillating-water-column wave energy converters and air turbines: A review," *Renewable Energy*, vol. 85, pp. 1391–1424, 2016. [Online]. Available: https://www.sciencedirect.com/science/article/pii/S0960148115301828

[2] A. Falcão and L. Gato, "8.05 - air turbines," in *Comprehensive Renewable Energy*, A. Sayigh, Ed. Oxford: Elsevier, 2012, pp. 111–149. [Online]. Available: https://www.sciencedirect.com/science/article/pii/B9780080878720008052

[3] T. Setoguchi and M. Takao, "Current status of self rectifying air turbines for wave energy conversion," *Energy Conversion and Management*, vol. 47, no. 15, pp. 2382–2396, 2006. [Online]. Available: https://www.sciencedirect.com/science/article/pii/S0196890405003158

[4] S. Raghunathan, "The wells air turbine for wave energy conversion," *Progress in Aerospace Sciences*, vol. 31, no. 4, pp. 335–386, 1995. [Online]. Available: https://www.sciencedirect.com/science/article/pii/037604219500001F

[5] T. Heath, "Chapter 334 - the development and installation of the limpet wave energy converter," in *World Renewable Energy Congress VI*, A. Sayigh, Ed. Oxford: Pergamon, 2000, pp. 1619–1622. [Online]. Available: https://www.sciencedirect.com/science/article/pii/B9780080438658503342

[6] M. INOUE, K. KANEKO, T. SETOGUCHI, and S. RAGHUNATHAN, "Simulation of starting characteristics of the wells turbine," in *4th Joint Fluid Mechanics, Plasma Dynamics and Lasers Conference*. American Institute of Aeronautics and Astronautics, may 1986. [Online]. Available: https://doi.org/10.2514%2F6.1986-1122

[7] M. Takao and T. Setoguchi, "Air turbines for wave energy conversion," *International Journal of Rotating Machinery*, vol. 2012, pp. 1–10, 2012. [Online]. Available: https://doi.org/10.1155%2F2012%2F717398

[8] T.-H. Kim, M. Takao, T. Setoguchi, K. Kaneko, and M. Inoue, "Performance comparison of turbines for wave power conversion," *International Journal of Thermal Sciences*, vol. 40, no. 7, pp. 681–689, 2001. [Online]. Available: https://www.sciencedirect.com/science/article/pii/S1290072901012571

[9] Y. Tujimoto, M. Shibata, S. Kouno, H. Hamakawa, H. Hayashi, and E. Kurihara, "Reduction of aerodynamic noise radiated from wells turbine," *IOP Conference Series: Earth and Environmental Science*, vol. 240, p. 052005, mar 2019. [Online]. Available: https://doi.org/10.1088%2F1755-1315%2F240%2F5%2F052005

[10] T. Ghisu, P. Puddu, F. Cambuli, and I. Virdis, "On the hysteretic behaviour of wells turbines," *Energy Procedia*, vol. 126, pp. 706–713, 2017, aTI 2017 - 72nd Conference of the Italian Thermal Machines Engineering Association. [Online]. Available: https://www.sciencedirect.com/science/article/pii/S187661021733816X

[11] T. K. Das, P. Halder, and A. Samad, "Optimal design of air turbines for oscillating water column wave energy systems: A review," *The International Journal of Ocean and Climate Systems*, vol. 8, no. 1, pp. 37–49, feb 2017. [Online]. Available: https://doi.org/10.1177%2F1759313117693639

[12] M. Torresi, M. Stefanizzi, F. Fornarelli, L. Gurnari, P. G. F. Filianoti, and S. M. Camporeale, "Performance characterization of a wells turbine under unsteady flow conditions," in *SECOND INTERNATIONAL CONFERENCE ON MATERIAL SCIENCE, SMART STRUCTURES AND APPLICATIONS: ICMSS-2019*. AIP Publishing, 2019. [Online]. Available: https://doi.org/10.1063%2F1.5138882

[13] V. Jayashankar, S. Anand, T. Geetha, S. Santhakumar, V. J. Kumar, M. Ravindran, T. Setoguchi, M. Takao, K. Toyota, and S. Nagata, "A twin unidirectional impulse turbine topology for OWC based wave energy plants," *Renewable Energy*, vol. 34, no. 3, pp. 692–698, mar 2009. [Online]. Available: https://doi.org/10.1016%2Fj.renene.2008.05.028

[14] T. Setoguchi, S. Santhakumar, H. Maeda, M. Takao, and K. Kaneko, "A review of impulse turbines for wave energy conversion," *Renewable Energy*, vol. 23, no. 2, pp. 261–292, jun 2001. [Online]. Available: https://doi.org/10.1016%2Fs0960-1481%2800%2900175-0

[15] A. Thakker and F. Hourigan, "Modeling and scaling of the impulse turbine for wave power applications," *Renewable Energy*, vol. 29, no. 3, pp. 305–317, mar 2004. [Online]. Available: https://doi.org/10.1016%2Fs0960-1481%2803%2900253-2

[16] D. Ferreira, L. Gato, and L. Eça, "Efficiency of biradial impulse turbines concerning rotor blade angle, guide-vane deflection and blockage," *Energy*, vol. 266, p. 126390, mar 2023. [Online]. Available: https://doi.org/10.1016%2Fj.energy.2022.126390

[17] M. Takao, Y. Kinoue, T. Setoguchi, T. Obayashi, and K. Kaneko, "Impulse turbine with self-pitch-controlled guide vanes for wave power conversion (effect of guide vane geometry on the performance)," *International Journal of Rotating Machinery*, vol. 6, no. 5, pp. 355–362, 2000. [Online]. Available: https://doi.org/10.1155%2Fs1023621x00000336

[18] A. Thakker, H. B. Khaleeq, M. Takao, and T. Setoguchi, "Effects of hub-to-tip ratio and reynolds number on the performance of impulse turbine for wave energy power plant," *KSME International Journal*, vol. 17, no. 11, pp. 1767–1774, nov 2003. [Online]. Available: https://doi.org/10.1007%2Fbf02983607

[19] C. Freeman, S. J. Herring, and K. Banks, "Impulse turbine for use in bi-directional flows," vol. US20100209236A1, jan 2008.

[20] L. Gato, A. Carrelhas, and A. Cunha, "Performance improvement of the axial self-rectifying impulse air-turbine for wave energy conversion by multi-row guide vanes: Design and experimental results," *Energy Conversion and Management*, vol. 243, p. 114305, sep 2021. [Online]. Available: https://doi.org/10.1016%2Fj.enconman.2021.114305

[21] A. Ponte, A. A. D. Carrelhas, L. M. C. Gato, J. C. C. Henriques, and A. F. O. Falcao, "Experimental study of a self-rectifying impulse axial-flow air turbine with fixed guide-vanes," *Proc. of 12th EWTEC*, pp. 1687–1–9, sep 2019.

[22] A. F. Falcão, J. C. Henriques, and L. M. Gato, "Self-rectifying air turbines for wave energy conversion: A comparative analysis," *Renewable and Sustainable Energy Reviews*, vol. 91, pp. 1231–1241, aug 2018. [Online]. Available: https://doi.org/10.1016%2Fj.rser.2018.04.019

[23] A. Carrelhas, L. Gato, J. Henriques, and A. Falcão, "Experimental study of a self-rectifying biradial air turbine with fixed guide-vanes arranged into two concentric annular rows," *Energy*, vol. 198, p. 117211, may 2020. [Online]. Available: https://doi.org/10.1016%2Fj.energy.2020.117211

[24] A. Falcão, L. Gato, and E. Nunes, "A novel radial self-rectifying air turbine for use in wave energy converters," *Renewable Energy*, vol. 50, pp. 289–298, feb 2013. [Online]. Available: https://doi.org/10.1016%2Fj.renene.2012.06.050

[25] A. Carrelhas, L. Gato, J. Henriques, A. Falcão, and J. Varandas, "Test results of a 30kW self-rectifying biradial air turbine-generator prototype," *Renewable and Sustainable Energy Reviews*, vol. 109, pp. 187–198, jul 2019. [Online]. Available: https://doi.org/10.1016%2Fj.rser.2019.04.008

[26] H. Maeda, S. Santhakumar, T. Setoguchi, M. Takao, Y. Kinoue, and K. Kaneko, "Performance of an impulse turbine with fixed guide vanes for wave power conversion," *Renewable Energy*, vol. 17, no. 4, pp. 533–547, aug 1999. [Online]. Available: https://doi.org/10.1016%2Fs0960-1481%2898%2900771-x

[27] T. Setoguchi, M. Takao, S. Santhakumar, and K. Kaneko, "Study of an impulse turbine for wave power conversion: Effects of reynolds number and hub-to-tip ratio on performance," *Journal of Offshore Mechanics and Arctic Engineering*, vol. 126, no. 2, pp. 137–140, may 2004. [Online]. Available: https://doi.org/10.1115%2F1.1710868